Petrographic analysis of crowded *Rosselia* ichnofabrics from the Tremadocian of Northwestern Argentina: Ethologic meaning and diagenesis

María DUPERRON[1] and Roberto A. SCASSO[1,2]

[1]CONICET-Universidad de Buenos Aires, Instituto de Geociencias Básicas, Aplicadas y Ambientales (IGEBA).

[2]Universidad de Buenos Aires, Facultad de Ciencias Exactas y Naturales, Departamento de Ciencias Geológicas, Ciudad Autónoma de Buenos Aires.

E-mails: maria.duperron@gmail.com, rscasso@gl.fcen.uba.ar.

ABSTRACT

Rosselia socialis were studied in the Ordovician Áspero Formation, in order to explore their sedimentary and diagenetic fingerprint in the substrate. These trace fossils are found forming crowded *Rosselia* ichnofabrics, described for the first time in pre-Quaternary strata of Argentina. We identified three microstructures corresponding to the central shaft complex, the burrow lining and the host rock of a trace fossil assigned to a terebellid polychaete. The infill of the central shaft complex represents downwards advection of surficial deposits located close to the burrow opening: fine-grained fecal mounds, and sandy mounds and lag deposits of manipulated, non-ingested material. Abundant phylosillicates in the central shaft complex and burrow lining evidence mechanical selection of particles with high specific surface area by the tracemaker. The fine-grained composition and multilayered organically bound structure of the burrow lining generate an impermeable and reinforced burrow, which combined with crowding grants physical and chemical stability to its inhabitants. This is especially advantageous in the high energy environments with shifting substrates where crowded *Rosselia* ichnofabrics are typically found. The central shaft complex and burrow lining are enriched in secondary iron minerals with respect to the host rock. Mineralized bacterial structures in the burrow lining evidence biologically induced precipitation of iron oxides and possibly sulphides. This coupled with the distribution of iron minerals in the burrow lining and central shaft complex suggests the occurrence of early diagenetic processes of organic matter decomposition and precipitation of authigenic iron minerals in *Rosselia* burrows, as observed in modern terebellid polychaetes.

Keywords: Terebellidae, deposit-feeders, Lower Ordovician, trace fossils, bioturbation.

RESUMEN

Análisis petrográfico de icnofábricas atestadas de Rosselia pertenecientes al Tremadociano del Noroeste Argentino: significado etológico y diagénesis.

Se estudiaron *Rosselia socialis* de la Formación Áspero (Ordovícico), donde forman icnofábricas densas, para explorar su marca sedimentológica y diagenética. Estas icnofábricas son descriptas por primera vez en estratos pre-Cuaternarios de la Argentina. Identificamos tres microestructuras correspondientes al complejo del canal central, el recubrimiento de la traza, y la roca hospedante de una traza fósil asignada a la acción de poliquetos terebélidos. El relleno del complejo del canal central refleja la advección hacia abajo de depósitos superficiales ubicados en torno a la abertura de la excavación: montículos fecales de grano fino, y montículos arenosos y *lags* conformados por material manipulado pero no ingerido. La abundancia de filosilicatos en el complejo del canal central y el recubrimiento de la traza evidencian selección mecánica de partículas de alta superficie específica por parte del productor. La composición de grano fino y el armazón multicapa orgánicamente ligado del recubrimiento de la traza generan una estructura impermeable y reforzada, que en combinación con una icnofábrica atestada garantizan estabilidad física y química al productor. El complejo del

canal central y recubrimiento de la traza están enriquecidos en minerales secundarios de hierro respecto a la roca. Las estructuras bacterianas mineralizadas del recubrimiento evidencian precipitación biológicamente inducida de óxidos de hierro y posiblemente de sulfuros. Esto, en conjunto con el enriquecimiento en minerales de hierro, sugiere descomposición de la materia orgánica durante la diagénesis temprana, con la consiguiente precipitación de minerales autigénicos de hierro en las excavaciones de *Rosselia*, tal como se observa en las de poliquetos terebélidos modernos.

Palabras clave: Terebellidae, depositívoros, Ordovícico Inferior, trazas fósiles, bioturbación.

INTRODUCTION

The ichnogenus *Rosselia* was first described from the Lower Devonian of Germany by Dahmer (1937), and since then it has been described in ancient successions ranging from the Early Cambrian to the Holocene (Häntzschel 1975, Nara and Haga 2007, Desjardins et al. 2010). Its ethology has been discussed by different authors, having been considered a dwelling structure of a sabellid polychaete with an associated impression of its tentacled crown (Dahmer 1937), the feeding structure of infaunal suspension-feeding animals (Chamberlain 1978, McCarthy 1979, Frey and Howard 1985), a feeding and sediment-stowage burrow (Frey and Howard 1990, MacEachern and Pemberton 1992, Pemberton et al. 1992), and a dwelling structure of a suspension-feeding animal which passively trapped muddy sediments (Nara 1995). Its formation by thalassinidean shrimps (Rindsberg and Gastaldo 1990), or by annelids or sea anemones (Suganuma et al. 1994) was also discussed. Nara (1995) concluded that the concentric structure of *Rosselia socialis* was formed due to outward expansion of muddy sediments selected from the surface sediments and accreted on to the burrow lining by a tentaculate detritus-feeding animal, similarly to the construction of fine-grained, concentrically laminated burrows by modern terebellid polychaetes (Rhoads 1967, Aller and Yingst 1978). Modern *Rosselia socialis*-like burrows can also be formed by polychaete worms belonging to the Spionidae and Cirratulidae Families (Gingras et al. 1999, 2008, Zorn et al. 2007, Olivero et al. 2012). These correspond to the sessile (or discretely motile), tentaculate, surface deposit-feeder polychaete guild (i.e., the 'terebellid way of life', Fauchald and Jumars 1979), which includes other families with similar behaviors like Amphareti-dae, or Trichobranchidae. Sabellidae, which correspond to the sessile, tentaculate, filter-feeder guild, also construct this sort of concentrically layered fine-grained burrow linings (Fauchald and Jumars 1979).

The present work analyzes *Rosselia socialis* belonging to shallow marine strata from the Late Cambrian - Ordovician Santa Victoria Group (Eastern Cordillera). We document for the first time the occurrence of crowded *Rosselia* ichnofabrics in pre-Quaternary strata of Argentina; the only other record corresponds to crowded *Rosselia*-like structures in Holocene deposits from Santa Cruz province (Olivero et al. 2012). As of yet, studies on *Rosselia* have not explored the imprint on the trace fossil of the particle-selection, biogenic reworking and diagenetic processes which characterize tentaculate, surface deposit-feeding polychaetes (Rhoads 1967, Aller and Yingst 1978, Fauchal and Jumars 1979, Jumars et al. 1982, Massé et al. 2019). In this work, we interpret the results of petrographic analysis in the light of the processes described in modern polychaetes to study the ethology of the *Rosselia* tracemaker and its sedimentological and diagenetic fingerprint on the substrate.

MATERIALS AND METHODS

The materials come from outcrops of the Áspero Formation in a single locality in Las Maderas Range, Jujuy province, Argentina. Large *Rosselia*-bearing blocks, belonging to 0.4–0.7 m thick beds interbedded with heterolithic shales, were inspected. The bed tops and soles were determined by diagnostic trace fossils present on the surfaces of the strata. Each face of these blocks was photographed and described in detail in the field in order to reconstruct the complex geometry of the trace fossils. Two large-sized samples were taken from crowded *Rosselia* ichnofabric-bearing sandstones, spanning the whole thickness of the bed; these contained 9 specimens of *Rosselia*.

Samples were cut and polished in sections longitudinal or transverse to the trace fossils to study the morphology and internal structure of the specimens. Iron-oxide- and moss-stained weathered surfaces were cleaned using 12.5 % (m/v) oxalic acid solution. The solution was applied with a paintbrush directly over stained surfaces; these were lightly scrubbed with a firm brush. The process was repeated 2-3 times until the surfaces were clean. Megascopic and microscopic (polarization microscope) observations allowed defining different

morphological elements on the basis of their color, texture, grain size, lamination, grain fabric, and presence of mineral precipitates. Coated samples were examined with a scanning electron microscope (SEM) Carl Zeiss NTS SUPRA 40 which belongs to the Centro de Microscopía Avanzada (CMA) of the Facultad de Ciencias Exactas y Naturales, University of Buenos Aires. Secondary electron (SE) imaging and backscattered-electron (BSE) imaging were utilized.

The morphological elements were grouped into three significant microstructures. They were described using standard petrographic parameters: texture, grain size, grain fabric (packing and grain orientation) and main components. The clay and fine-silt fraction, dominated by phyllosilicates, was classified as 'epimatrix' (Dickinson 1970) because it was not possible to discern if it consists of recrystallized detrital matrix or authigenic phyllosilicate minerals (i.e., cement). The grain size distribution was quantified by image analysis on thin section photographs; these were taken at small, millimetric intervals in vertical succession, and all the clast sections in each photograph were digitally drawn and measured. The proportion of main components (clasts and interstitial constituents, disaggregated into the epimatrix and cements) was quantified by point counting. As the proportion of voids was very low, porosity was not quantified.

GEOLOGIC AND SEDIMENTOLOGIC SETTING

The studied succession belongs to the Cordillera Oriental (Eastern Andean Cordillera) of Northwestern Argentina, characterized by the metasedimentary basement of Puncoviscana Complex (Turner 1960, Zimmerman 2005) and the sedimentary rocks of the Cambrian Mesón Group and Late Cambrian - Ordovician Santa Victoria Group (Turner 1960). The present study focuses on the shallow marine deposits of the Áspero Formation (late Tremadocian) of the Santa Victoria Group in the area of Las Maderas Range (Fig. 1a); this formation is equivalent to the Humacha Member of the Santa Rosita Formation (Moya 1988, Buatois and Mángano 2003).

The Áspero Formation in the area of Las Maderas Range is characterized by intercalations of horizontally laminated sandstone and heterolithic intervals deposited in a shallow subtidal to intertidal, mixed-energy estuarine system (Duperron et al. 2018, Duperron and Scasso 2020, Fig. 1). Three subenvironments have been recognized: a storm-dominated outer bay, a middle bay characterized by tidal flats and channels with rare storm deposits, and a river-dominated bay-head delta (Duper-

ron and Scasso 2020). The intervals where the *Rosselia* beds (Fig. 2) are found correspond to the wave-dominated outer bay, which is characterized by high-energy sandy and bioclastic deposits showing hummocky and swaley cross stratification and parallel lamination, intercalated with wave-rippled tidal flat facies. *Rosselia socialis* occur in sandstone beds bearing sigmoidal and tabular cross-stratification, current-ripple and parallel lamination, with internal discontinuities and intraclast-rich surfaces (Fig. 2b, f). Other trace fossils belonging to the *Cruziana* and *Skolithos* ichnofacies appear commonly in the base of the sandstone beds (Fig. 2c): these correspond to a pre-depositional suite of horizontal trilobite traces (*Dimorphichnus, Monomorphichnus, Cruziana*) which are cross-cut by a post-depositional suite of vermiform vertical traces (*Diplocraterion, Skolithos, Arenicolites*; Duperron and Scasso 2020).

RESULTS

Morphology of *Rosselia socialis*

The studied specimens consist of concentrically layered, funnel-shaped endichnial burrows. The funnels are up to 40 cm long, with a diameter ranging from 2 to 5 cm; some burrows show swellings giving them a slightly spindled shape. Burrow cross-sections overlap and crosscut each other in several instances in the bed tops, reaching up to 10 cm in width (Fig. 2a). Generally, the burrows are oriented vertically (Figs. 2b, d and 3), although some appear to be slightly oblique (Fig. 3d). In some specimens, the internal structure is modified by secondary smaller-scale bioturbation structures which give a swirly massive appearance to the burrow (Figs. 2e and 3c, i.e. Uchman and Krenmayr 1995); in these cases, vertically oriented muscovite flakes reveal the relict original grain fabric of *Rosselia socialis*. The secondary bioturbation structures consist of vermiform trace fossils 1 mm-thick oriented chaotically (Fig. 2e).

Five morphological elements were identified in *Rosselia socialis* (Fig. 3e): the central shaft complex; the burrow lining (inner part of the wall); the iron-stained outer surface of the burrow lining; the light-colored outer part of the wall; and the host rock immediately beside the burrow. The central shaft complex (Figs. 3 and 4), approximately 1 cm in diameter, is composed of one or more mica-coated tubular structures infilled by sand (Fig. 3a-c).It is surrounded by dark gray, muddy, mica-rich, concentrically laminated burrow lining with a sinuous and crinkly appearance (Fig. 3a-d), with a total width of 1-2 cm. The iron-stained outer surface of the burrow lining is massive and black due to iron-oxide cementation (Fig.
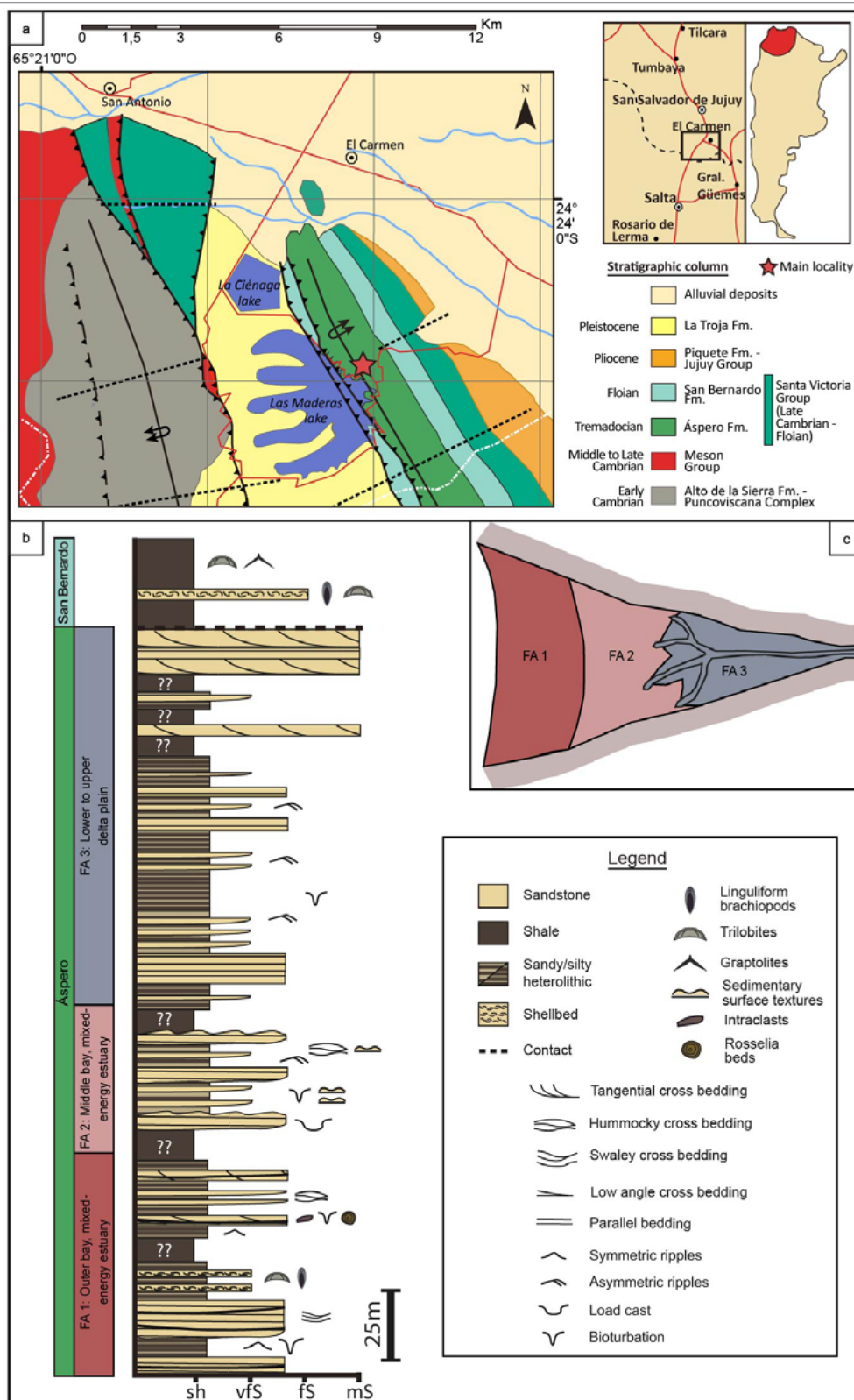
Figure 1. a) Geological map of Las Maderas Ranges. The stratigraphic interval where the *Rosselia* specimens were collected belongs to the Áspero Formation, which crops out on the western flank of Las Maderas Range. Modified after Duperron et al. (2018); b) Integrated sedimentologic column for Las Maderas Range and facies associations, Duperron and Scasso (2020); c) Distribution of facies associations in the mixed-energy estuary: outer bay (FA1), middle bay (FA2), bay-head delta (FA3). Duperron and Scasso (2020), modified after Dalrymple et al. (1992).

3a, c-d), and shows in some cases transversal striae. The light-colored outer wall consist of a narrow (0.2-0.8 cm) sandy zone adjacent to the burrow lining characterized by vertically arranged reddish pink to orange laminae (Figs. 2d-e, 3a, c-d and 4a); it contrasts with the darker-colored host rock, and

with the black iron-stained outer surface of the burrow lining. The primary lamination observed in the host rock bends downwards in proximity to the burrow wall; the affected area overlaps partially or completely with the light-colored outer wall (Figs. 3c-d and 4a).
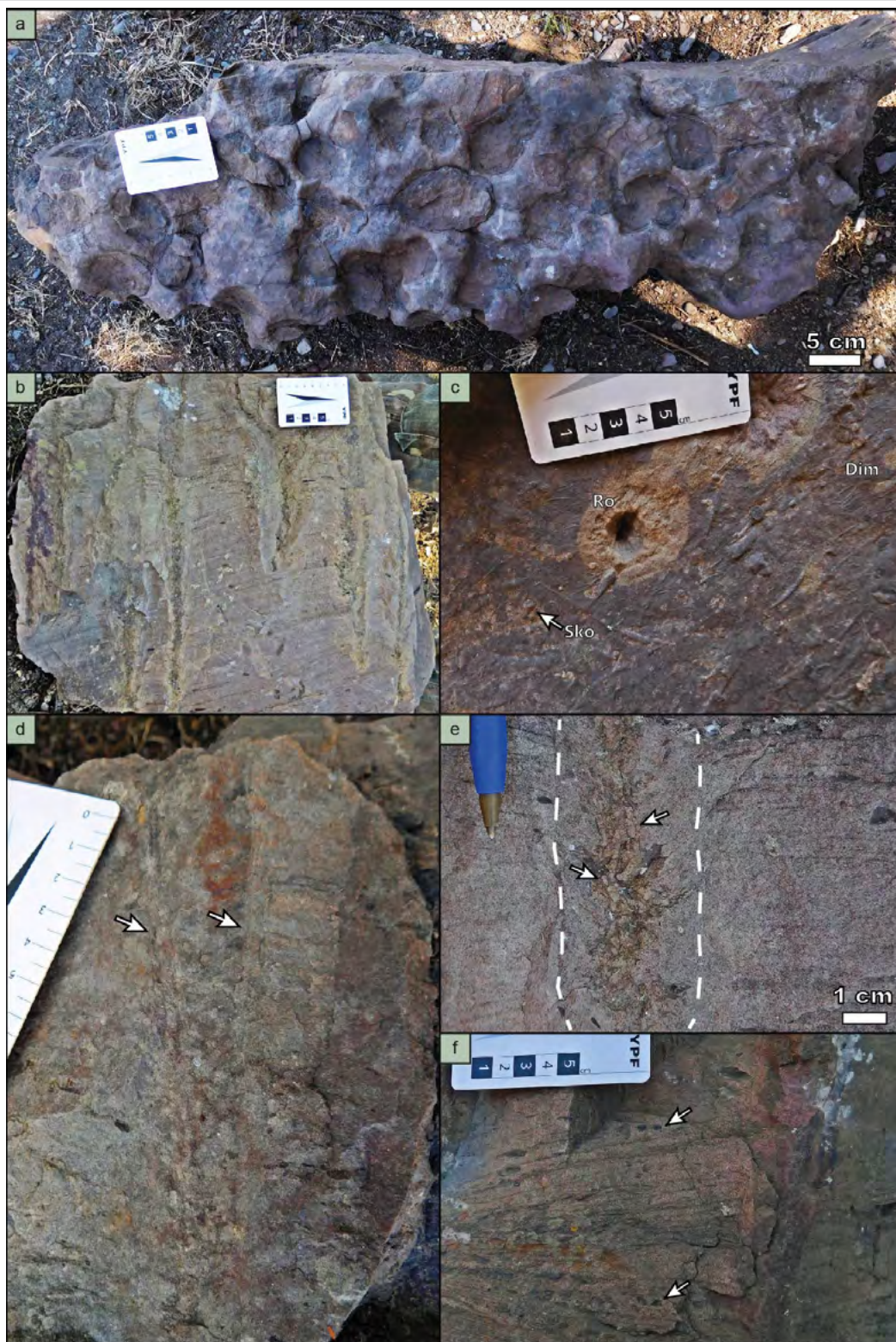
Figure 2. *Rosselia* beds, bedding planes and vertical sections. The stratigraphic up corresponds to the upper part of the photograph in vertical sections. The ruler is in cm increments. a) Upper bedding plane. The surface is uneven with a trough and dome topography formed respectively by eroded *Rosselia* cross-sections and undisturbed sandstone; b) Vertical section, showing closely spaced *Rosselia* specimens 20-40 cm long in tabular, cross-bedded sandstone; c) Lower bedding plane of *Rosselia* bed, showing *Dimorphichnus* isp. (Dim), *Skolithos* isp. (Sko; burrow shaft, white arrow), *Rosselia socialis* (Ro) with an alteration halo; d) Detail of a *Rosselia socialis* specimen: the burrow has a massive aspect with an indistinguishable structure in contrast to the laminated host rock, but an outer rim is clearly visible which likely corresponds to the outer wall of the burrow (white arrows); e) Detail of a *Rosselia socialis* specimen with an outer sand-rich massive area (dotted line) and an inner muddy area which is reworked by abundant small vermiform structures (white arrows); f) Intraclast-rich laminae in the host rock (white arrows).

Microstructures: grain size, composition and microfabric

The five morphological elements described previously were grouped into three significative microstructures on the basis of their sediment composition and gran size distribution: the central shaft complex, burrow lining and host rock (Fig. 5).

Central shaft complex: The central shaft complex is composed by one or more associated sandy tubular structures (Fig. 4a-b). The margins of each of these are demarcated by
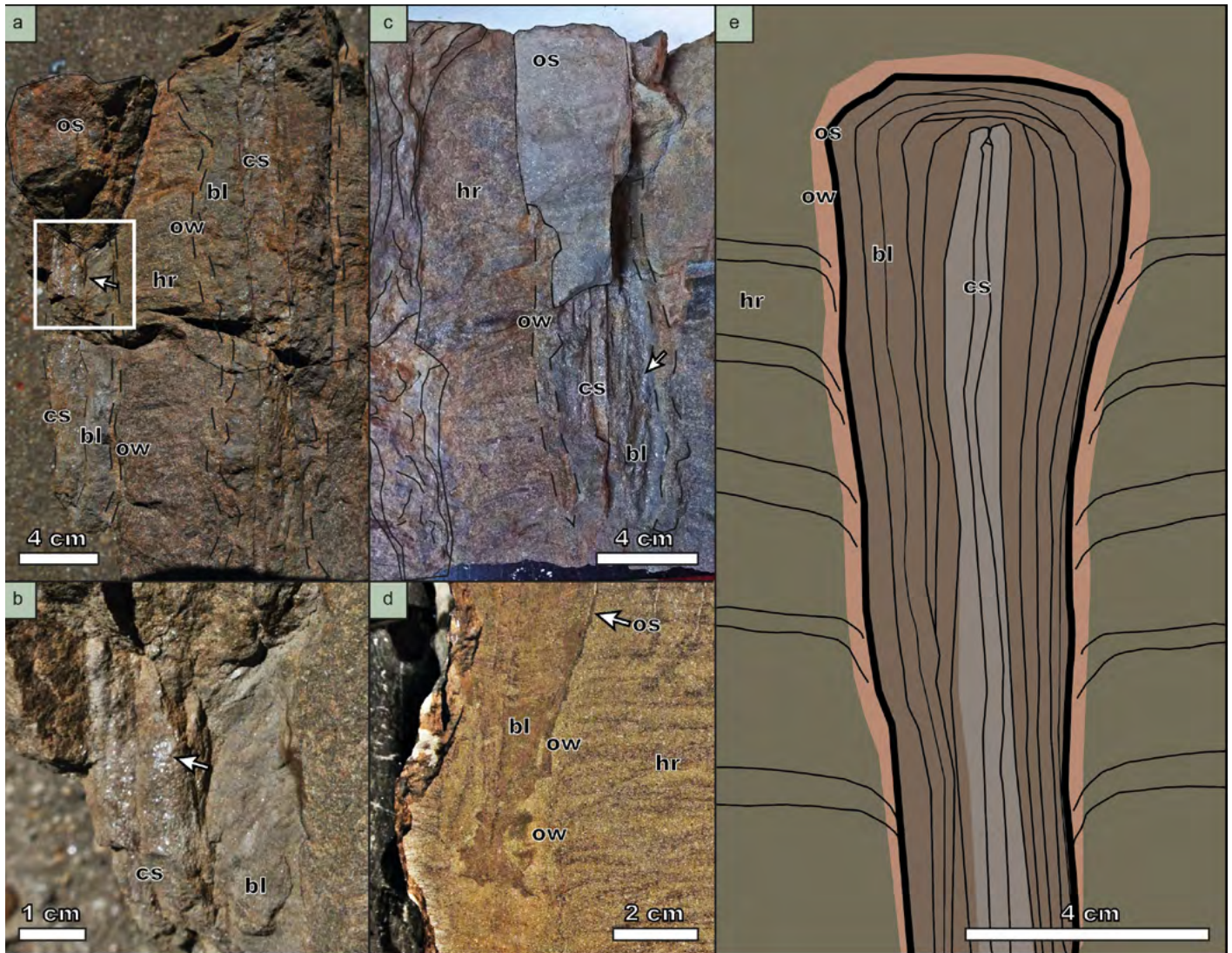
Figure 3. Morphology of *Rosselia* specimens: a) Two funnel-shaped burrows, showing the sandy, mica-rich central shaft complex (cs, arrow) surrounded by the muddy, dark-gray mica-rich burrow lining (bl) showing massive or crude concentrical lamination. The outer surface of the burrow lining (os) is almost black, with a massive appearance due to iron-oxide cementation. The outer wall (ow, dashed line) adjacent to the burrow lining and the host rock (hr)consists of a narrow, lighter-colored sandy zone; b) Inset of "a" showing the central shaft complex (cs), composed by one or more sandy, mica-coated tubular structures (arrow), surrounded by the muddy burrow lining (bl); c) Two *Rosselia* specimens, with the internal structure outlined. The specimen on the right shows the central shaft complex (cs), crude concentrically-laminated burrow lining (bl), iron-stained outer surface of the burrow lining (os), the light-colored outer wall (ow) and the host rock (hr). Intense bioturbation gives a massive appearance to the burrow on the left. The arrow points to a specially mica-rich zone in the burrow lining; d) Section of an oblique *Rosselia* burrow, showing the muddy burrow lining (bl), iron-stained outer surface (white arrow, os) and the sandy, light-colored outer wall (ow). The primary lamination of the host rock (hr) bends downwards in proximity to the burrow; e) Schematic drawing of the morphology of the *Rosselia* specimens studied and the adjacent host rock, showing the central shaft complex (cs), concentrically laminated burrow lining (bl), massive iron-stained outer surface (os), light-colored outer wall (ow) and the host rock (hr).

fine-grained laminae with vertically oriented grains, rimmed by small aggregates of iron oxides or stylolitic iron-oxide precipitates (Fig. 4b).

The infill of the shafts is characterized by the alternation of quartz-rich coarser-grained laminae and finer-grained laminae with a higher proportion of chloritic epimatrix (Fig. 4b-c). Coarser-grained laminae show clast-supported fabrics with tangential to concavo-convex contacts, and finer-grained laminae show matrix-supported fabrics with floating grains; the clasts are oriented parallel to the lamination. The frame-

work grains (48.6 %, Table 1), relatively more abundant in the coarser-grained laminae, show a grain size mode in very fine sand (Fig. 5a-b) with a mean grain diameter of 84 µm. They are composed dominantly by monocrystalline quartz, followed by polycrystalline quartz, orthoclase, plagioclase, volcanic and metamorphic lithic grains, and scarce glauconite; muscovite and biotite flakes are relatively abundant in the central shaft complex, representing 9 % of the framework grains. Medium and coarse sand grains consisting of muddy intraclasts, phosphatic bioclasts and concretions are present
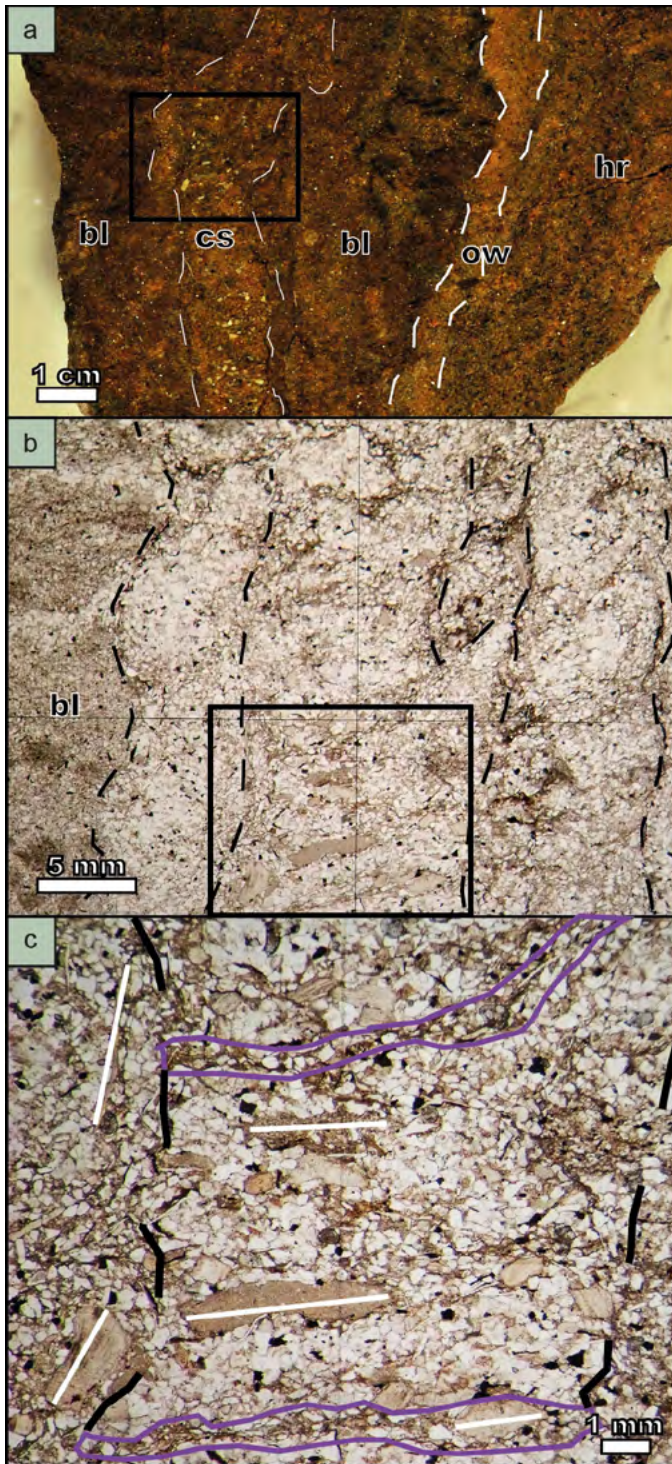
Figure 4. Microphotographs of the central shaft complex: a) Polished section of a *Rosselia* burrow showing the sandy central shaft complex (cs), muddy burrow lining (bl), light-colored outer wall (ow) and the host rock (hr). The central shaft complex is characterized by the relative abundance of medium to coarse-grained sand clasts; b) Thin section microphotography (inset of "a"), showing sandy central shaft complex composed of several tubular structures. These are demarcated by fine-grained margins (black dashed lines) with two kinds of iron oxide cement: stylolitic precipitates and small aggregates of iron minerals. To the left, the muddy burrow lining (bl) can be seen; c) Close-up of a tubular structure (inset of "b"), showing sandy fill with grain fabric parallel to the lamination and intercalated fine grained muddy laminae (purple outline). Medium to coarse-sized grains are relatively abundant. The shaft margins are marked by fine-grained, vertical laminae with vertical grain fabric (left and right zones of the picture, dashed line). White lines inside clasts illustrate the predominant grain fabric.

quartz overgrowth appears in minority and occurs dominantly in the sandy laminae. Four kinds of iron oxide precipitates can be distinguished in the central shaft complex. The first kind are small grains or aggregates disseminated throughout the structure (Fig. 6a), consisting of individual or clumped, circular to subcircular mineral aggregates with a 1 to 30-μm diameter. Some grains with irregular and angular shapes are present, which might correspond to replaced organic matter particles. This kind of precipitate occurs also in the margins of some of the shafts in the central shaft complex, which are rimmed by fine-grained, matrix-rich laminae with abundant, small-sized opaque mineral aggregates (Fig. 4b). The second kind consists of patches of opaque mineral aggregates with a clumpy aspect, which occur as replacement of biotite crystals and lithic fragments or associated with the chloritic epimatrix (Fig. 6b-c). The third kind consists of stylolitic, amorphous cement concentrated along isolated vertical fractures (Fig. 6d). These fractures run parallel to the burrow structure (Fig. 6d), concentrating along the fine-grained margins of the central shaft complex (Fig. 4b), or at the outer surface of the burrow lining. The fourth kind consists of diffuse red-tinted patches, commonly associated with the second or third kind of precipitates (Fig. 6d).

Burrow lining: The dominant primary fabric of the burrow lining consists of concentric lamination arranged parallel or slightly oblique to the central shaft complex, with vertically oriented grains (Figs. 5c and 7). Laminae are composed of silt- to clay-sized particles, with abundant muscovite and iron-replaced biotite and lithoclasts (Figs. 5c and 7); the grain size and amount of clay minerals, muscovite and iron oxide vary within different laminae. Secondary, smaller-scale vermiform bioturbation structures (Fig. 7a-b) modify the primary fabric produced by the *Rosselia* tracemaker. These structures are infilled by matrix-poor very-fine sand; the adjacent grains in the fine-grained *Rosselia* burrow lining are oriented parallel to the margins of the secondary vermiform structures (Fig. 7b).

as secondary components. The finer-grained laminae are composed of the same framework grains, with a higher proportion of chloritic epimatrix and muscovite and biotite flakes. The interstitial materials (51.4 %) are composed of chloritic epimatrix (26.3 %), iron oxide cement (23.3 %) and quartz overgrowth cement (1.8 %, Table 1). The epimatrix consists of chlorite rims of irregular width composed of green and brown chlorites with a heterogeneous, murky aspect. Syntaxial

Figure 5. Thin section microphotographs and histograms of the central shaft complex (a-b), burrow lining (c-d) and host rock (e-f) microstructures. The scale bar of the microphotographs is 500 μm. The histograms show the grain size distribution of the clastic fraction and percentages of the main components. >mS - medium sand and coarser grains, fS - fine sand, vfS - very fine sand, cSi - coarse silt, Cla - clasts, Chl – chloritic epimatrix, Fe - iron oxide cement. Minor quartz overgrowth is not represented.
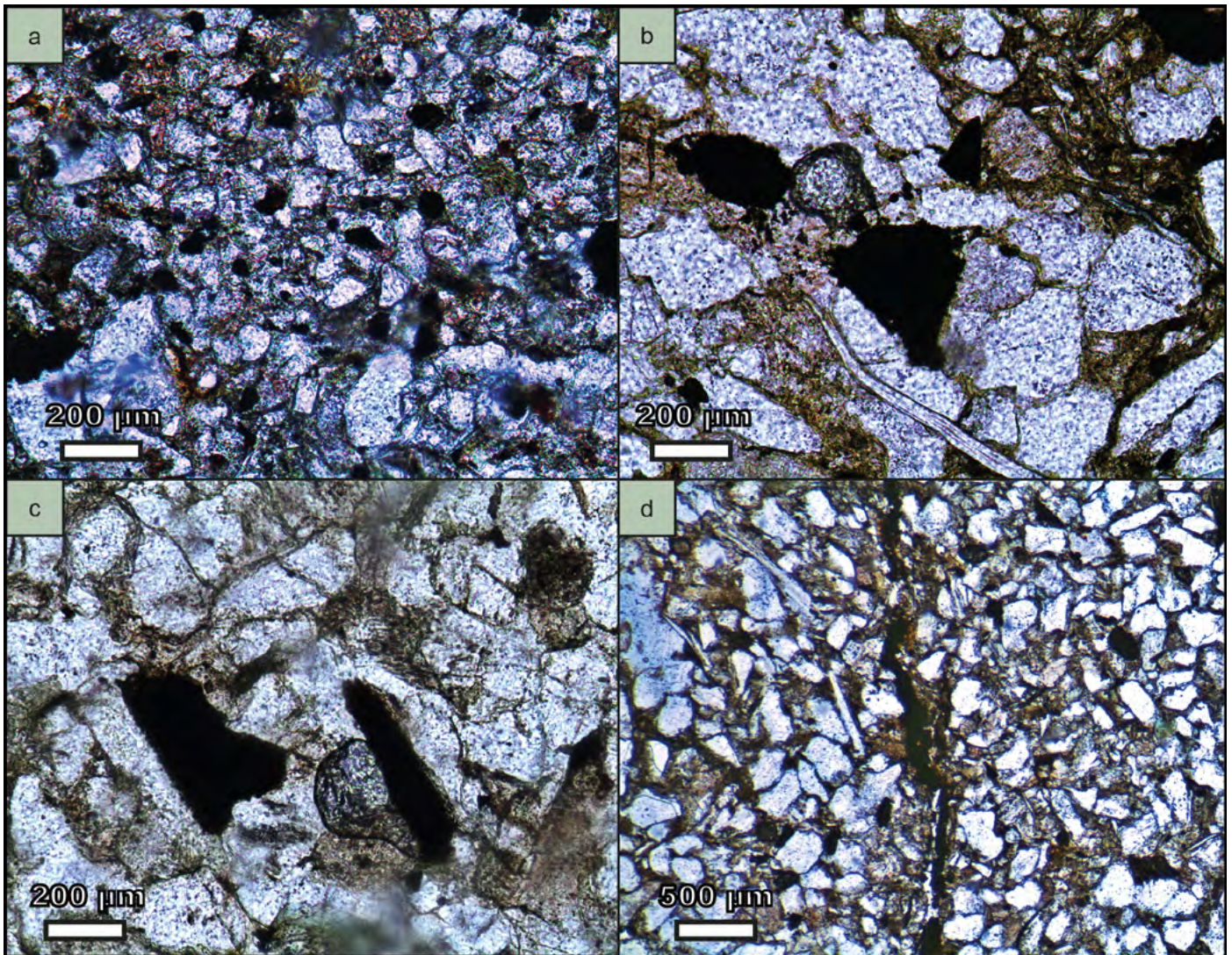
Figure 6. Different kinds of iron-oxide and opaque minerals: a) Individual or clumped, circular to subcircular mineral aggregates; b) Opaque mineral aggregates with a clumpy aspect partially replacing lithic clasts in the central shaft complex; c) Patchy iron oxides replacing biotite and other mafic grains in the host rock; d) Stylolitic, amorphous iron cement concentrated along isolated fractures, associated with diffuse red iron-oxide patches.

Table 1. Proportion of the main components in the central shaft complex, burrow lining and host rock microstructures. The proportion of interstitial constituents is disaggregated into epimatrix, iron oxide cement and quartz overgrowth cement.

Proportion of the main components in the microstructures	Central shaft complex (%) n = 528	Burrow lining (%) n = 455	Host rock (%) n = 410
Clasts	48.6	40.2	63.8
Interstitial constituents	51.4	59.8	36.2
Epimatrix	26.3	29.2	21.0
Iron oxide cement	23.3	30.5	12.7
Quartz overgrowth cement	1.8	0.0	2.5

In the burrow lining the grain fabric is matrix- to clast-supported with tangential to straight grain contacts and isolated floating grains; the clasts are oriented vertically with respect to the lamination. Framework grains (40.2 %, Table 1) show a mean grain diameter of 41 μm (Fig. 5c-d); they consist of dominant monocrystalline quartz followed by orthoclase and plagioclase, with polycrystalline quartz, volcanic and metamorphic lithic grains as secondary components; muscovite

and biotite flakes are relatively abundant, representing 7 % of the framework grains. The interstitial material (59.8 %) is formed by a mixture of chloritic epimatrix (29.2 %) with iron oxide cement (30.5 %, Table 1) forming disseminated aggregates, patches, stylolitic cements (Figs. 5c and 7c), and replacing lithoclasts and biotite.

SEM imaging of the burrow lining showed local associations of nanometric to micrometric-scale structures (Fig. 8) consisting of smooth and rugged spherical structures, discoidal structures, and twisted filaments embedded in the rock. The spherical structures (Fig. 8a, c-g) range between 300–1000 nm in diameter, the smooth forms being smaller than the rugged ones. The spheres commonly show small bridges binding them with the rock (Fig. 8d-e). Adjoined spheres have also been observed (Fig. 8c). Smooth discoidal structures (Fig. 8a, c-d, g), characterized by depressions in their central area, range between 300–500 nm in diameter. Twisted filaments (Fig. 8a-b, e-f) are 100–150 nm in width and up to 8 μm in length. In BSE images, rugged spherical structures and twisted filaments show moderate contrast with the background (Fig. 8f) while smooth spheres and discoidal structures show no contrast (Fig. 8h).

Host rock: The lamination is composed of alternating quartz-rich, matrix-poor, coarser-grained laminae and muscovite-rich, matrix-rich, finer-grained laminae with patchy iron-oxide cementation (Fig. 7a, c). In both kinds of laminae, the grain fabric is clast-supported with straight to concavo-convex contacts; the clasts are oriented horizontally to obliquely with respect to the lamination. Framework grains (63.8 %, Table 1) show a mode in very fine sand, with a mean grain diameter of 97 μm (Fig. 5e-f). They are composed dominantly by monocrystalline quartz, followed by polycrystalline quartz, orthoclase, plagioclase, volcanic and metamorphic lithic grains, and scarce glauconite; muscovite and biotite form 3 % of the clastic fraction. The interstitial material (36.2 %) is dominated by a chloritic epimatrix (21 %), which consists of chlorite rims of irregular width composed of brown and green chlorite with a murky, heterogeneous aspect; these are concentrated in the finer-grained laminae. The cement consists of iron-oxide cement (12.7 %) and quartz overgrowth (2.5 %, Table 1). The former predominates in coarser-grained, sandy laminae and the latter in finer-grained, mica-rich laminae. There are two kinds of iron-oxide cements. Patchy cement occurs in association with replaced biotite crystals and lithic fragments and with chloritic epimatrix (Fig. 6c), bridging in some cases the interstitial space between these components; the patches are commonly aligned with the grain fabric, and approximate-
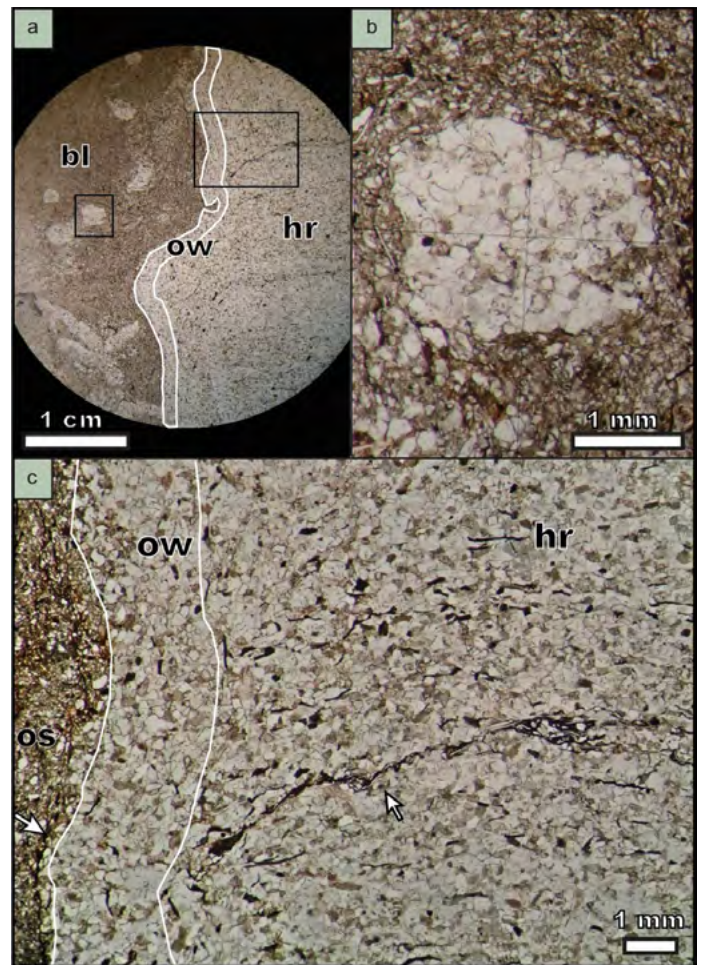
Figure 7. a) Microphotograph of bioturbated burrow lining (bl), outer wall (ow) and host rock (hr); b) Inset of "a" showing sand-filled vermiform structure within the muddy burrow lining. The phylosillicates of the muddy burrow lining are oriented concentrically around the vermiform structure; c) Inset of "a" showing the outer surface of the burrow lining (os) with localized iron-oxide precipitation and stylolitic cement (arrow); the iron-depleted outer wall (ow) with vertical grain fabric with respect to the stratification; and the host rock (hr) with downwards bending lamination and oblique to vertical grain fabric near the outer wall. Iron-oxide and opaque minerals in the host rock are concentrated along isolated fractures and aligned mafic grains, oriented approximately parallel to the primary lamination (arrow) and grain fabric.

ly parallel to the lamination. The stylolitic cement appears along isolated fractures, which are also oriented parallel to the lamination (Fig. 7c).

Between the burrow lining and the host rock lies a narrow zone characterized by vertical grain fabric (Fig. 7c). This zone shows lower proportion of iron minerals than the surrounding host rock. Lithic clasts and biotite flakes are partially or completely dissolved and replaced by iron-oxide and clay minerals, resulting in "reddish relict clasts". This area corresponds to the light-colored outer wall described earlier (Figs. 3a, c-d and 4a).
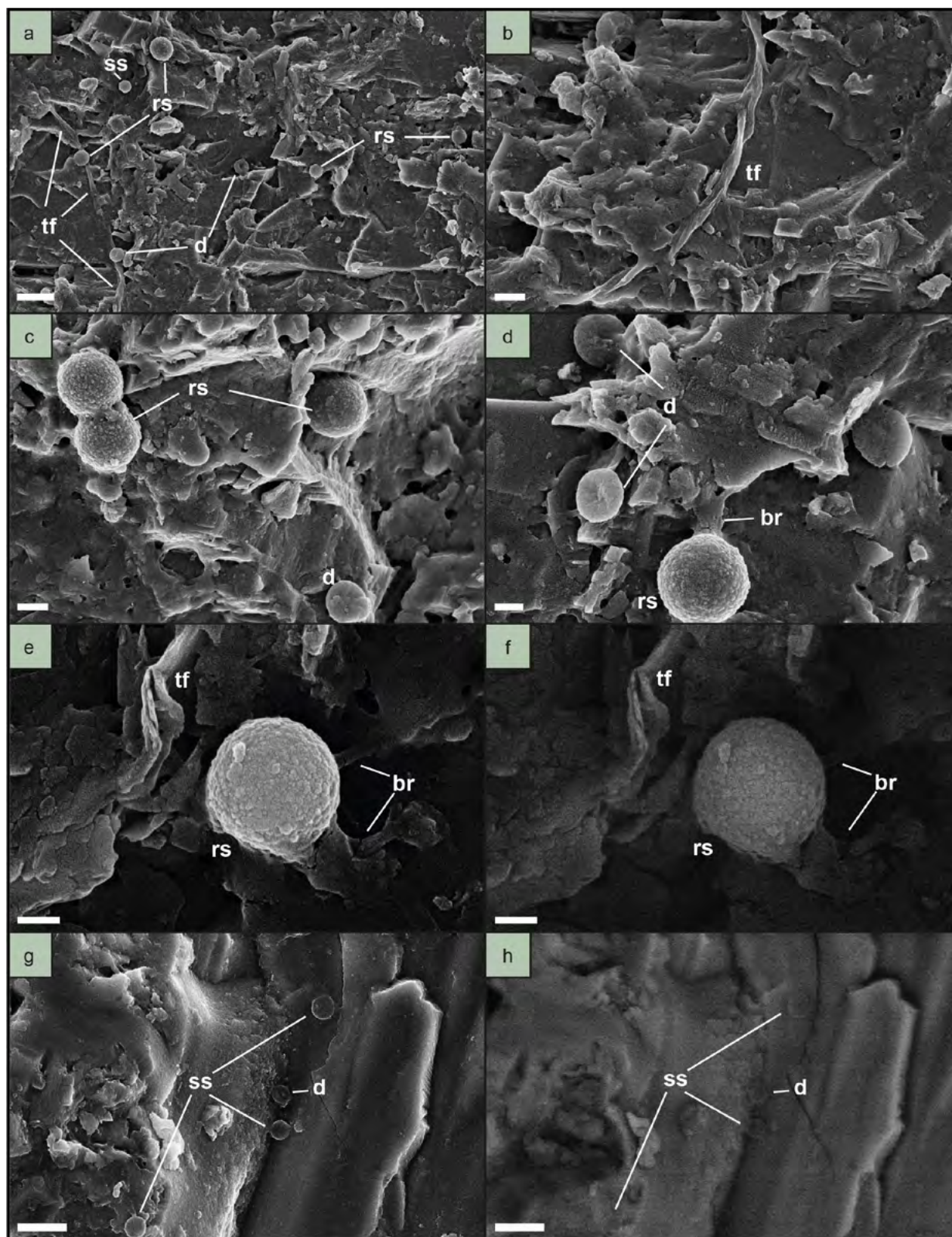
Figure 8. SEM images of the burrow lining, showing association of nanometric to micrometric-scale structures with interpreted morphological biosignatures: a) Association of smooth and rugged spherical structures (ss and rs, respectively), smooth discoidal structures (d), and a twisted filament (tf). Scale bar: 1 μm; b) Closer view of a twisted filament (tf) embedded in the cement. Scale bar: 300 nm; c) Rugged spherical structures (rs) and a discoidal structure (d). Scale bar: 300 nm; d) Discoidal structures (d) and a rugged spherical structure (rs) bound to the rock with a small bridge (br). Scale bar: 300 nm; e) Rugged spherical structures (rs) with small bridges (br), and twisted filament (tf). Scale bar: 200 nm; f) BSE image of e., showing moderate contrast of the rugged sphere with respect to the background. Scale bar: 200 nm; g) Smooth spherical structures (ss) and discoidal structures (d). Scale bar: 1 μm; h) BSE image of g., showing lack of contrast of smooth spheres and discoidal structures with respect to the background. Scale bar: 1 μm.

DISCUSSION

Rosselia ethology

Three morphological elements correlative to the sediments associated with modern polychaete worms were identified in the studied *Rosselia socialis:* (a) the central shaft complex, (b) the burrow lining, and (c) the host rock (representing undisturbed sediments). (a) and (b) correspond to distinct microstructures characterized by their sediment composition and grain-size distribution (Fig. 5), evidencing biogenic reworking by the *Rosselia* tracemaker. The remaining morphological elements –the iron-stained outer surface of the burrow lining and the light-colored outer wall– probably reflect diagenetic processes (see discussion below).

The central shaft complex is characterized by a broad range of grain sizes, from coarse silt to coarse-grained sand (Fig. 5b); this contrasts with the host rock sediments, which show better sorting and scarcity of medium to coarse sand grains (Fig. 5f). The bulk grain size distribution shown in figure 5b represents the combination of the finer-grained laminae, the sandy coarser-grained laminae and the isolated medium to coarse sand grains which make up the infill of the shafts (Fig. 4). The alternation between sandier, coarser-grained laminae and muddier, finer-grained laminae in the central shaft complex might be interpreted as a passive fill reflecting the sedimentary variations registered in the host rock; however, the central shaft complex and the host rock microstructures differ significantly both in their grain size distribution and composition (Fig. 5), indicating that the sediments which infill the lumen are somehow modified with respect to the normal sedimentation. In modern tentaculate, surface deposit-feeding polychaete worms, the following surface sediment deposits have been described surrounding the burrow opening: (1) muddy, fine-grained fecal mounds (reflecting the preference of clay- to fine silt-sized sediments for feeding due to their greater contents of organic detritus and bacterial coatings – Taghon et al. 1978–); (2) coarser-grained mounds and lag deposits of large particles (consisting of sediments which were manipulated by the worm but discarded for feeding or tube-building); and (3) even coarser-grained prospected areas depleted of fine-grained sediments (Rhoads 1967, Aller and Yingst 1978, Massé et al. 2019). In *Amphitrite ornata*, periodical infilling of the burrow opening by these sediments causes the worm to perform upwards thrusts meant to expel them (Rhoads 1967). The infill of the lumen might thus correspond to gravitational, downwards advection of part of these surface deposits. We interpret then that the fine-grained laminae in the central shaft complex represent material from the muddy fecal mounds,

and the sandier laminae and isolated coarser grains the manipulated, non-ingested sediments. The latter medium to very coarse sand fraction is composed exclusively of intrabasinal constituents (intraclasts, phosphatic bioclasts and concretions), which reflects the dynamics of this estuarine environment where coarser-grained siliciclastics imported from the continent were retained at the bay head delta (Duperron and Scasso 2020). Additionally, the central shaft complex –as well as the burrow lining– is significantly enriched in muscovite and biotite flakes when compared to the host rock (Fig. 3a-c); this evidences mechanical selection of large-surface, low-density particles by the mucus-secreting tentacles of the worms (Jumars et al. 1982, Self and Jumars 1988, Guieb et al. 2004).

The burrow lining consists of concentric laminae accreted during the lifetime of the trace-maker. These are enriched in chloritic epimatrix with respect to the host rock (Fig. 5d, f), reflecting concentration of the original fine-grained detrital clays (transformed into chloritic rims during diagenesis) by the *Rosselia* trace-maker. These fine sediments were specifically gathered and sorted from the surrounding surface sediments to build the tube, as occurs in the burrows of *Amphitrite ornata* (Rhoads 1967, Aller and Yingst 1978). Slight variations in grain size and composition between the laminae likely reflect fluctuations in the available surface sediments (Aller and Yingst 1978, Nara 1995). In *Rosselia socialis* and modern *Rosselia*-like burrows regular, concentrically laminated structures are generally accepted to be originated by the accretion of sediments on the inner part of the wall, generating successions of newer lining which displace, expand and split the older ones, compacting nearby sediments as well (Aller and Yingst 1978, Seilacher 1986, 2007, Nara 1995). This has been hypothesized to reflect moult-like behavior caused by the growth of the tracemaker (Aller and Yingst 1978, Nara 1995). Accordingly, in stacked *Rosselia* the width of the central shaft should be progressively larger from one bulb to the overlying one reflecting each period of growth (e.g. the *Rosselia* specimens illustrated in figure 3 of Nara 1997). However, most existing works on equilibrium *Rosselia* seem to indicate that this is not frequent (Nara 1995, 2002, Buatois et al. 2016, Campbell et al. 2016) and the width of *Rosselia* central shafts has been measured and described as constant by Netto et al. (2014). In these cases, the multilayer structure of *Rosselia* must have another origin.

In *Amphitrite ornata* a voluminous, multilayered organically bound structure built with fine-grained sediments generates a relatively impermeable burrow, which presents low diffusive permeability with respect to other species of marine tube-dwellers (Aller 1983). Low-permeability walls shelter the

burrow microenvironment from adverse chemical conditions in the surrounding anoxic sediments, where the oxic layer reaches a few centimeters depth at the most (Jørgensen 1982, Kristensen 2000); this maintains physico-chemical parameters within the range of physiological tolerance of its inhabitant (Aller 1982, Kristensen and Kotska 2005). They also help to lower irrigation efforts, and to reduce changes in burrow water composition during intertidal periods; increasing burrow size or decreasing inter-burrow distance are alternative strategies for achieving the same results (Aller 1982). The fine-grained, multi-layered structure of *Rosselia* probably acts as a buffer against the adverse chemical environment in the surrounding anoxic sediments and in some cases against chemical changes produced by variations in the influx of seawater to the burrow (i.e. during intertidal periods, Aller and Yingst 1978). On the other hand, the strongly reinforced concentrical structure must present greater physical resistance than simpler burrow linings (as occurs in the tubes of *Cirriformia luxuriosa*, Zorn et al. 2010). Thus, building a concentrical structure made of fine-grained sediments is probably aimed to grant isolation from the surrounding anoxic sediments and physical stability to the Ordovician *Rosselia* builders.

Crowded *Rosselia* ichnofabrics have been interpreted as a stress-tolerant suite developed under conditions of relatively high energy, sedimentation rates and organic matter input, tolerated by the *Rosselia* tracemakers but not by the normal marine communities; they are interpreted to represent a strategic behavior of organisms adapted to chronically stressed environments (Nara 2002, Netto et al. 2014). The high densities and monospecific character of crowded *Rosselia* ichnofabrics would thus represent a normal feature of stress-tolerant suites (Netto et al. 2014). However, crowding has been shown to represent in itself an effective strategy for physically stabilizing the substrate against erosion (Schäfer 1972, Rhoads et al. 1978, Aller 1982). This effect would be highly beneficial in the high-energy environments with shifting substrates where crowded *Rosselia* ichnofabrics are commonly found (Netto et al. 2014) and might thus represent one of the adaptations which allowed the *Rosselia* tracemakers to thrive.

In summary, the fine-grained, multilayered constructive design of the Ordovician *Rosselia* coupled with the development of crowded *Rosselia* ichnofabrics provided chemical and physical stability to the burrows. These behaviors might represent important adaptations which allowed communities of polychaete worms to colonize the unconsolidated, highly shifting intertidal to shallow subtidal substrates of the Áspero Formation (Duperron and Scasso 2020). The buffering capa-

bility of *Rosselia*-type burrows might represent an additional advantage in chemically adverse or fluctuating environments like the proximal delta front facies described by Campbell et al. (2016) or the estuarine environment of the Áspero Formation (Duperron and Scasso 2020).

Early diagenesis in *Rosselia socialis*

Iron-oxide cementation on the exterior of *Rosselia* burrows has been described as common by Uchman and Krenmayr (1995). In *Rosselia* from the Áspero Formation the central shaft complex and burrow lining are significantly enriched in iron oxide cement with respect to the host rock (Fig. 5), representing early diagenetic iron mineral mobilization and precipitation focused in the burrow. Partial or complete replacement of iron-rich clasts such as biotite flakes and mafic lithoclasts by clumpy aggregates of iron minerals (Fig. 6b-c) reflects the transformation of reactive iron present on the original grains. The enhanced diagenesis in the burrow and its vicinity might be explained in two ways: the burrow might have acted as a biogeochemical microenvironment which favored the precipitation of authigenic minerals, or this precipitation might have been entirely abiogenic and controlled by the petrophysical characteristics of the burrow. In any of these cases, the initial iron minerals were modified during later diagenesis and exhumation of the rocks as it is shown by the oxidation of iron minerals and the generation of stylolitic cement in the burrow and surrounding sediments (Figs. 6d and 7c).

Iron oxide precipitation around the burrow might have been controlled by abiogenic processes, linked with the strong permeability contrast between the burrow and the host rock and with the resulting permeability anisotropy. This might be caused both by the contrasting composition and grain size of the burrow lining and the host rock (Fig. 5), and by the change in the grain fabric around the burrow lining (Fig. 7). Contrasting grain size between shale and sandstone beds or smaller-scale sedimentary bodies or structures (like mud drapes or mud chips), as well as grain fabric heterogeneity related to certain sedimentary structures like cross-bedding, control permeability values and anisotropy in sandstone reservoirs (dos Anjos et al. 2000, Huysmans et al. 2008, Morad et al. 2010). Calcite cementation has been shown to be influenced by this kind of permeability heterogeneities, with peripheral cementation (i.e., cement surrounding a sedimentary body) being developed around interfaces between lithofacies with contrasting petrophysical characteristics like mudstone-sandstone ones (Moraes and Surdam 1993, dos Anjos et al. 2000, Pomar et al. 2004). This type of cementation has been related to focused flow of diagenetic fluids around such interfaces (McBride et

al. 1995, Pomar et al. 2004). The massive, iron-stained outer surface of the burrow lining (Figs. 3 and 7) might very well be explained by peripheral iron oxide cementation controlled by the petrophysical characteristics of the burrow and its contrast with the host rock. Part of the iron might have been supplied by leaching of the adjacent light-colored outer wall, evidenced by the lower abundance of iron minerals in that area (Figs. 3 and 7), and by the alteration of iron-rich clasts (Fig. 6b, c). The stylolitic cement (Figs. 6d and 7c) found in the burrow lining, central shaft complex and host rock can also be produced by focused flow of diagenetic fluids following the grain fabric and fracture zones, although this would necessary be produced during telogenesis. However, the scattered iron-oxide precipitates and replaced mafic lithoclasts concentrated within the burrow lining and central shaft complex (Figs. 4, 6a and 7c) show no preferred orientation or distribution (except for the rims in the central shaft complex), and thus they do not appear to be strongly influenced by the grain fabric or by the contrasting grain size between the two microstructures. Their formation is harder to explain by pure abiogenic mechanisms related to the petrophysical characteristics of the burrow.

On the other hand, the iron-oxide mineralization in the burrows might have been controlled by a biogeochemical microenvironment which favored the precipitation of authigenic minerals. For example, in the case of *Amphitrite ornata* (Aller and Yingst 1978), the polychaete's burrow acts as a site of intense organic matter concentration and decomposition, and authigenic mineral formation. The accretion of multiple generations of mucus-lined, fine-grained burrow lining creates a three-dimensional body rich in organic matter and reactive metals (as these compounds associate preferentially with fine-grained sediments, Aller 1982). This fosters an intense anaerobic metabolic activity, generating a microenvironment characterized by the formation of authigenic minerals linked with sulphate reduction such as elemental sulfur, pyrite or other solid phase sulfides. Metallic elements like iron, manganese and zinc are thus mobilized and concentrated in the burrow lining with respect to the surrounding sediments (Aller and Yingst 1978). The distribution of iron oxides in the studied *Rosselia* specimens might reflect the same processes: the disseminated iron mineral aggregates (Fig. 6a) may have nucleated around decomposing organic matter dispersed throughout the burrow, while the rims of small aggregates in the central shaft complex (Fig. 4b) might represent the degradation of the organic lining on the inner burrow lining and its replacement by iron sulphides and/or elemental sulfur (i.e., Olivero and López Cabrera, 2010). The replacement of iron-rich clasts in the burrow (Fig. 6b-c) could be produced by their

reaction with the reduced sulfates generated by bacterial metabolism. The association of nanometric to micrometric-scale structures observed in the burrow lining of *Rosselia* (Fig. 8) shows a series of morphological characteristics indicative of a microbial origin and of bacterially induced precipitation of authigenic minerals; their presence supports the hypothesis of iron mineral precipitation caused by the specific biogeochemical microenvironment within the burrow. Smooth spherical structures fall within the size-range of small coccoid bacterial cells (0.05 - 2μm, Westall 1999). Rugged spheres and twisted stalks showing moderate contrast in BSE images (Fig. 8e-f) reflect higher-density materials with respect to the rock; this suggests that their composition is rich in heavy elements like metals, and that these structures are mineralized to a higher degree than non-contrasting, smooth spheres and discs (Fig. 8g-h). Rugged spheres might represent encrusted bacteria overgrown by mineral aggregates which nucleated on the surface of the cells (i.e., McKenzie and Vasconcelos 2009, Gleeson et al. 2012) or extracellular mineral aggregates (i.e., Labrenz et al. 2000); both kinds of aggregates are most likely produced by active or passive biologically induced precipitation. Their consistently larger size with respect to smooth forms, and the presence of adjoined forms resembling bacteria undergoing cellular division (i.e., Westall 1999, Gleeson et al. 2012), support the first option. The bridges which join the rugged spheres with the rock probably represent EPS secreted by bacteria (MacLean et al. 2008, Gleeson et al. 2012). Discoid forms do not resemble any known bacterial cellular morphology, but possibly represent deceased, collapsed bacteria (i.e. Ma et al. 2014, Cushnie et al. 2016). Twisted filaments probably represent twisted stalks, a characteristic biosignature produced exclusively by iron-oxidizing microaerophilic bacteria (Ehrenberg 1836, Chan et al. 2011, Picard et al. 2015). These consist of extracelular mineral aggregates composed of iron oxides, excreted by the bacteria as a by-product of their metabolism (Chan et al. 2011, Picard et al. 2015). In summary, we interpret the presence of two kinds of structures: poorly mineralized structures consisting of coccoid bacteria including collapsed cells (smooth spheres and discoid forms) and more heavily mineralized structures produced by biologically induced precipitation (rugged spheres and twisted filaments). Rugged spheres are morphologically similar to and fall slightly below the size range of biologically induced spherules of titanium sulfide (Labrenz et al. 2000) and elemental sulfur (Gleeson et al. 2012) which occur in association with sulfate-reducing bacteria in modern biofilms; on the other hand, their size range is one order of magnitude below the one reported for typical pyrite framboids (Sawlo-

wicz 1993, Wilkin et al. 1996). Thus, these structures might be formed by solid phase sulphides or elemental sulfur, but not by pyrite. Iron-oxidizing, iron-reducing and sulfate-reducing bacteria have been shown to coexist and contribute to iron cycling in coastal and shallow marine environments (Laufer et al. 2016); the observed structures produced by iron-oxidizing and potentially by sulfate-reducing bacteria might correspond to such an association.

Considering the distribution of iron oxide precipitates concentrated within the burrow lining and central shaft complex and the presence of microstructures evidencing bacterial action and biologically induced precipitation of authigenic minerals (including iron oxides and possibly sulphides), we interpret that biologically controlled early diagenetic processes like the ones recorded in modern *Amphitrite ornata* burrows are the most likely cause for the iron mineral cementation observed in the studied *Rosselia* specimens. This first diagenetic stage has probably been overprinted by telogenetic iron remobilization.

CONCLUSIONS

Rosselia socialis of the Early Ordovician Áspero Formation (Northwestern Argentina) were found forming crowded *Rosselia* ichnofabrics, documented for the first time in pre-Quaternary strata of Argentina. Through their petrographic analysis and their comparison with structures described in modern polychaetes, we arrived at the following conclusions:

The infill of the central shaft complex reflects downwards advection of surficial deposits generated by the deposit feeding activity of the tracemaker: muddy, fine-grained fecal mounds, and coarser-grained mounds and lag deposits of manipulated, non-ingested material.

The muddy burrow lining is formed by silt and very fine sand-sized sediments, selected and transported to the subsurface by the tracemaker. The choice of fine-grained sediments and a voluminous, multilayered organically bound structure generates a relatively impermeable and reinforced burrow, which combined with crowding grants physical and chemical stability to the burrow. This is especially advantageous in the high energy environments with shifting substrates where crowded *Rosselia* ichnofabrics are typically found.

The central shaft complex and muddy burrow lining are enriched in iron mineral precipitates with respect to the host rock. Mineralized bacterial structures in the burrow lining evidence biologically induced precipitation of iron oxides and possibly solid phase sulphides. Their presence along with the distribution of the iron mineral precipitates suggests early diagenetic processes involving anaerobic organic matter decomposition and precipitation of authigenic iron minerals, as observed in modern terebellid polychaete burrows.

REFERENCES

Aller, R.C. 1982. The effects of macrobenthos on chemical properties of marine sediment and overlying water. In: McCall, P.L. and Tevesz, M. J.S. (eds.), Animal-sediment relations: The biogenic alteration of sediments. Plenum Press: 53-102, New York.

Aller, R.C. 1983. The importance of the diffusive permeability of animal burrow linings in determining marine sediment chemistry. Journal of marine Research 41(2): 299-322.

Aller, R.C. and Yingst, J.Y. 1978. Biogeochemistry of tube-dwellings: a study of the sedentary polychaete *Amphitrite ornata* (Leidy). Journal of Marine Research 36: 201-254.

Buatois, L.A. and Mángano, M.G. 2003. Sedimentary facies, depositional evolution of the Upper Cambrian–Lower Ordovician Santa Rosita formation in northwest Argentina. Journal of South American Earth Sciences 16(5): 343-363.

Buatois, L.A., García-Ramos, J.C., Piñuela, L., Mángano, M.G. and Rodríguez-Tovar, F.J. 2016. *Rosselia socialis* from the Ordovician of Asturias (northern Spain) and the early evolution of equilibrium behavior in polychaetes. Ichnos 23(1-2): 147-155.

Campbell, S.G., Botterill, S.E., Gingras, M.K. and MacEachern, J.A. 2016. Event sedimentation, deposition rate, and paleoenvironment using crowded *Rosselia* assemblages of the Blue sky Formation, Alberta, Canada. Journal of Sedimentary Research 86(4): 380-393.

Chamberlain, C.K. 1978. Recognition of trace fossils in cores. In: Basan,

P.B. (ed.), Trace Fossil Concepts. SEPM Short Course 5: 119-166, Tulsa.

Chan, C.S., Fakra, S.C., Emerson, D., Fleming, E.J. and Edwards, K.J. 2011. Lithotrophic iron-oxidizing bacteria produce organic stalks to control mineral growth: implications for biosignature formation. The ISME journal 5(4): 717-727.

Cushnie, T.T., O'Driscoll, N.H. and Lamb, A.J. 2016. Morphological and ultrastructural changes in bacterial cells as an indicator of antibacterial mechanism of action. Cellular and molecular life sciences 73(23): 4471-4492.

Dahmer, G. 1937. Lebensspuren aus dem Taunusquarzit und den Siegener Schichten (Unterdevon). Preussische Geologische Landesanstalt zu Berlin 1936(57): 523-539.

Dalrymple, R.W., Zaitlin, B.A. and Boyd, R. 1992. Estuarine facies models: conceptual basis and stratigraphic implications. Journal of Sedimentary Research, 62(2):1130-1146.

Desjardins, P.R., Gabriela Mángano, M., Buatois, L.A. and Pratt, B.R. 2010. *Skolithos* pipe rock and associated ichnofabrics from the southern Rocky Mountains, Canada: colonization trends and environmental controls in an early Cambrian sand-sheet complex. Lethaia 43(4): 507-528.

Dickinson, W.R. 1970. Interpreting detrital modes of graywacke and arkose. Journal of Sedimentary Research 40(2): 695-707.

dos Anjos, S.M., De Ros, L.F., de Souza, R.S., de Assis Silva, C.M. and Sombra, C.L. 2000. Depositional and diagenetic controls on the reservoir quality of Lower Cretaceous Pendencia sandstones, Potiguar rift basin, Brazil. AAPG Bulletin 84(11): 1719-1742.

Duperron, M., Scasso, R.A. and Moya, M.C. 2018. Geología del área del Embalse Las Maderas, provincia de Jujuy, con referencia a las acumulaciones bioclásticas fosfáticas del Tremadociano y Floiano. Revista de la Asociación Geológica Argentina 75(1): 95-114.

Duperron, M. and Scasso R.A. 2020. Paleoenvironmental significance of microbial mat-related structures and ichnofaunas in an Ordovician mixed-energy estuary. Áspero Formation of Santa Victoria Group, Northwestern Argentina. Journal of Sedimentary Research: in press.

Ehrenberg, C.G. 1836. Vorläufige Mitteilungen über das wirkliche Vorkommen fossiler Infusorien und ihre grosse Verbreitung. Poggendorf Annalen 38: 213-227.

Fauchald, K. and Jumars, P.A. 1979. The diet of worms: a study of polychaete feeding guilds. Oceanography and marine Biology annual review 17: 193-284.

Frey, R.W. and Howard, J.D. 1985. Trace fossils from the Panther Member, Star Point Formation (Upper Cretaceous), Coal Creek Canyon, Utah. Journal of Paleontology 59(2): 370-404.

Frey, R.W. and Howard, J.D. 1990. Trace fossils and depositional sequences in a clastic shelf setting, Upper Cretaceous of Utah. Journal of Paleontology 64(5): 803-820.

Gingras, M.K., Pemberton, S.G., Saunders, T. and Clifton, H.E. 1999. The ichnology of modern and Pleistocene brackish-water deposits at Willapa Bay, Washington; variability in estuarine settings. Palaios 14(4): 352-374.

Gingras, M.K., Dashtgard, S.E., MacEachern, J.A. and Pemberton, S.G. 2008. Biology of shallow marine ichnology: a modern perspective. Aquatic Biology 2(3): 255-268.

Gleeson, D.F., Pappalardo, R.T., Anderson, M.S., Grasby, S.E., Mielke, R.E., Wright, K.E. and Templeton, A.S. 2012. Biosignature detection at an Arctic analog to Europa. Astrobiology 12(2): 135-150.

Guieb, R.A., Jumars, P.A. and Self, R.F. 2004. Adhesive-based selection by a tentacle-feeding polychaete for particle size, shape and bacterial coating in silt and sand. Journal of Marine Research 62(2): 260-281.

Häntzschel, W. 1975: Trace fossils and problematica. In: Teichert, C. (ed.): Treatise on Invertebrate Paleontology, W, Miscellanea. Geological Society of America and University of Kansas Press, 269 pp. Lawrence.

Huysmans, M., Peeters, L., Moermans, G. and Dassargues, A. 2008. Relating small-scale sedimentary structures and permeability in a cross-bedded aquifer. Journal of Hydrology 361(1-2): 41-51.

Jørgensen, B.B. 1982. Ecology of the bacteria of the sulphur cycle with special reference to anoxic—oxic interface environments. Philosophical Transactions of the Royal Society of London B298 (1093): 543-561.

Jumars, P.A., Self, R.F. and Nowell, A.R. 1982. Mechanics of particle selection by tentaculate deposit-feeders. Journal of Experimental Marine Biology and Ecology 64(1): 47-70.

Kristensen, E. 2000. Organic matter diagenesis at the oxic/anoxic interface in coastal marine sediments, with emphasis on the role of burrowing animals. Hydrobiologia 426(1): 1-24.

Kristensen, E. and Kostka, J.E. 2005. Macrofaunal burrows and irrigation in marine sediment: microbiological and biogeochemical interactions. In: Kristensen, E., Haese, R.R. and Kostka, J.E. (eds.), Interactions between macro–and microorganisms in marine sediments. American Geophysical Union Coastal and Estuarine Studies 60: 125-157, Washington.

Labrenz, M., Druschel, G.K., Thomsen-Ebert, T., Gilbert, B., Welch, S.A., Kemner, K.M., Logan, G.A., Summons, R.E., De Stasio, G., Bond, P.L., Lai, B., Kelly, S.D. and Banfield, J.F. 2000. Formation of sphalerite (ZnS) deposits in natural biofilms of sulfate-reducing bacteria. Science 290(5497): 1744-1747.

Laufer, K., Nordhoff, M., Røy, H., Schmidt, C., Behrens, S., Jørgensen, B.B. and Kappler, A. 2016. Coexistence of microaerophilic, nitrate-reducing, and phototrophic Fe (II) oxidizers and Fe (III) reducers in coastal marine sediment. Applied and Environmental. Microbiology 82(5): 1433-1447.

Ma, S., Li, H., Yan, C., Wang, D., Li, H., Xia, X., Dong, X., Zhao, Y., Sun, T., Hu, P. and Guan, W. 2014. Antagonistic effect of protein extracts from *Streptococcus sanguinis* on pathogenic bacteria and fungi of the oral cavity. Experimental and Therapeutic Medicine 7(6): 1486-1494.

MacEachern, J.A. and Pemberton, S.G. 1992. Ichnological aspects of Cretaceous shoreface successions and shoreface variability in the Western Interior Seaway of North America. In: Pemberton, S.G. (ed.), Application of Ichnology to Petroleum Exploration. SEPM Core Workshop 17: 57-84, Tulsa.

MacLean, L.C., Tyliszczak, T., Gilbert, P.U., Zhou, D., Pray, T.J., Onstott, T.C. and Southam, G. 2008. A high-resolution chemical and structural study of framboidal pyrite formed within a low-temperature bacterial biofilm. Geobiology 6: 471-480.

Massé, C., Garabetian, F., Deflandre, B., Maire, O., Costes, L., Mesmer-Dudons, N., Duchênet, J.C., Bernard, G., Grémare, A. and Ciutat, A. 2019. Feeding ethology and surface sediment reworking by the ampharetid polychaete *Melinna palmata* Grube, 1870: Effects on sediment characteristics and aerobic bacterial community composition. Journal of Experimental Marine Biology and Ecology 512: 63-77.

McBride, E.F., Milliken, K.L., Cavazza, W., Cibin, U., Fontana, D., Picard, M.D. and Zuffa, G.G. 1995. Heterogeneous distribution of calcite cement at the outcrop scale in Tertiary sandstones, northern Apennines, Italy. AAPG Bulletin 79(7): 1044-1062.

McCarthy, B. 1979. Trace fossils from a Permian shoreface-foreshore environment, eastern Australia. Journal of Paleontology 53(2): 345-366.

McKenzie, J.A. and Vasconcelos, C. 2009. Dolomite Mountains and the origin of the dolomite rock of which they mainly consist: historical developments and new perspectives. Sedimentology 56(1): 205-219.

Morad, S., Al-Ramadan, K., Ketzer, J.M. and De Ros, L.F. 2010. The impact of diagenesis on the heterogeneity of sandstone reservoirs: A review of the role of depositional facies and sequence stratigraphy. AAPG Bulletin 94(8): 1267-1309.

Moraes, M.A. and Surdam, R.C. 1993. Diagenetic heterogeneity and reservoir quality: Fluvial, deltaic, and turbiditic sandstone reservoirs, Potiguar and Reconcavo rift basins, Brazil. AAPG Bulletin 77(7): 1142-1158.

Moya, M.C. 1988. Lower Ordovician in the Southern Part of the Argentine Eastern Cordillera. In: Bahlburg, H., Breitkreuz, C. and Giese, P. (eds.), The Southern Central Andes, Springer, Lecture Notes in Earth Sciences 17: 55-69, Berlin Heidelberg.

Nara, M. 1995. *Rosselia socialis*: a dwelling structure of a probable terebellid polychaete. Lethaia 28(2): 171-178.

Nara, M. 1997. High-resolution analytical method for event sedimentation using *Rosselia socialis*. Palaios 12(5): 489-494.

Nara, M. 2002. Crowded *Rosselia socialis* in Pleistocene inner shelf deposits: benthic paleoecology during rapid sea-level rise. Palaios 17(3): 268-276.

Nara, M. and Haga, M. 2007. The youngest record of trace fossil *Rosselia socialis*: Occurrence in the Holocene shallow marine deposits of Japan. Paleontological Research 11(1): 21-28.

Netto, R.G., Tognoli, F.M., Assine, M. L. and Nara, M. 2014. Crowded *Rosselia* ichnofabric in the Early Devonian of Brazil: an example of strategic behavior. Palaeogeography, Palaeoclimatology, Palaeoecology 395: 107-113.

Olivero, E.B. and López Cabrera, M.I. 2010. *Tasselia ordamensis:* A biogenic structure of probable deposit-feeding and gardening maldanid polychaetes. Palaeogeography, Palaeoclimatology, Palaeoecology 292(1-2): 336-348.

Olivero, E.B., López Cabrera, M.I., Ercolano, B., Pittaluga, S. and Lizarralde, Z. 2012. Caught in fraganti: Actual and Holocene, crowded *Rosselia*-like mud-lined tubes produced by spionid polychates. Ameghiniana Suplemento - Resúmenes 49(4): R152.

Pemberton, S.G., Van Wagoner, J.C. and Wach, G.D. 1992: Ichnofacies of a wave-dominated shoreline. In: Pemberton, S.G. (ed.), Application of Ichnology to Petroleum Exploration. SEPM Core Workshop 17: 339-382, Tulsa.

Picard, A., Kappler, A., Schmid, G., Quaroni, L. and Obst, M. 2015. Experimental diagenesis of organo-mineral structures formed by microaerophilic Fe (II)-oxidizing bacteria. Nature Communications 6: 6277.

Pomar, L., Westphal, H. and Obrador, A. 2004. Oriented calcite concretions in Upper Miocene carbonate rocks of Menorca, Spain: evidence for fluid flow through a heterogeneous porous system. Geologica Acta 2(4): 271-284.

Rhoads, D.C. 1967. Biogenic graded bedding. Journal of Sedimentary Research 35(4): 461-476.

Rhoads, D.C., Yingst, J.Y. and Ullman, W.J. 1978. Seafloor stability in central Long Island Sound: Part I. Temporal changes in erodibility of fine-grained sediment. In: Wiley, M.L. (ed.), Estuarine interactions. Academic Press: 221-244, New York.

Rindsberg, A.K. and Gastaldo, R.A. 1990. New insight on ichnogenus *Rosselia* (Cretaceous and Holocene, Alabama). Journal of the Alabama Academy of Science 61: 154.

Sawlowicz, Z. 1993. Pyrite framboids and their development: a new conceptual mechanism. Geologische Rundschau 82(1): 148-156.

Schäfer, W. 1972, Ecology and Paleoecology of Marine Environments. In: Craig, G.Y. (ed.); University of Chicago Press, Chicago, 568 p., Chicago.

Seilacher, A. 1986. Evolution of behaviour as expressed in marine trace fossils. In: Nitecki, M.H. and Kitchell, J.A. (eds.), Evolution of Animal Behaviour. Oxford University Press: 67–87, New York.

Seilacher, A. 2007. Trace fossil analysis. Springer Science and Business Media.

Self, R.F. and Jumars, P.A. 1988. Cross-phyletic patterns of particle selection by deposit feeders. Journal of Marine Research 46(1): 119-143.

Suganuma, K., Omori, M., Hirakoso, S. and Ryuugasaki Collaborative Research Group. 1994. On the ichnogenus *Rosselia*, fossil burrows found from the Kamiiwahashi Formation, in the district of Tokizaki, Edosakimachi, Ryuugasaki City, Ibaraki Prefecture. Journal of Fossil Research 26: 61-68.

Taghon, G.L., Self, R.F. and Jumars, P.A. 1978. Predicting particle selection by deposit feeders: A model and its implications 1. Limnology and Oceanography 23(4): 752-759.

Turner, J.C.M. 1960. Estratigrafía de la Sierra de Santa Victoria y adyacencias. Boletín de la Academia Nacional de Ciencias de Córdoba 41: 165-196.

Uchman, A. and Krenmayr, H.G. 1995. Trace fossils from lower Miocene (Ottnangian) molasse deposits of Upper Austria. Paläontologische Zeitschrift 69 (3-4): 503-524.

Westall, F. 1999. The nature of fossil bacteria: a guide to the search for extraterrestrial life. Journal of Geophysical Research E104: 16437-16451.

Wilkin, R.T., Barnes, H.L. and Brantley, S.L. 1996. The size distribution of framboidal pyrite in modern sediments: an indicator of redox conditions. Geochimica et cosmochimica acta 60(20): 3897-3912.

Zimmermann, U. 2005. Provenance studies of very low-to low-grade metasedimentary rocks of the Puncoviscana complex, northwest Argentina. Geological Society Special Publications 246(1): 381-416, London.

Zorn, M.E., Muehlenbachs, K., Gingras, M.K., Konhauser, K.O., Pemberton, S.G. and Evoy, R. 2007. Stable isotopic analysis reveals evidence for groundwater-sediment-animal interactions in a marginal-marine setting. Palaios 22(5): 546-553.

Zorn, M.E., Gingras, M.K. and Pemberton, S.G. 2010. Variation in burrow-wall micromorphologies of select intertidal invertebrates along the Pacific Northwest coast, USA: behavioral and diagenetic implications. Palaios 25(1): 59-72.